

1           **Strategies for merging Microbial Fuel Cell Technologies in Water**  
2           **Desalination processes: start-up protocol and desalination efficiency**  
3           **assessment**

4  
5           **Zulema Borjas<sup>1</sup>, Abraham Esteve-Núñez<sup>1,2</sup> and Juan Manuel Ortiz<sup>1,3\*</sup>**

6           <sup>1</sup> Madrid Institute for Advanced Studies Water. Scientific-Technological Park of Alcalá, Madrid 28805, Spain;  
7           zulema.borjas@imdea.org

8           <sup>2</sup> Department of Chemical Engineering, University of Alcalá, Madrid 28871, Spain; [abraham.esteve@uah.es](mailto:abraham.esteve@uah.es)

9           <sup>3</sup> FCC Aqualia, Gestión Integral del Agua S.A., FCC Citizen Services. Avenida del Camino de Santiago, 40,  
10           Building 3, 4th Floor, 28050, Madrid (Spain)

11  
12           \* Corresponding author: [juanma.ortiz@imdea.org](mailto:juanma.ortiz@imdea.org); Tel.: +34-918 30 59 62-  
13

14           **Abstract**

15           Microbial Desalination Cells constitute an innovative technology where microbial fuel  
16           cell and electro dialysis merge in the same device for obtaining fresh water from saline  
17           water with no energy-associated cost for the user. In this work, an anodic biofilm of the  
18           electroactive bacteria *Geobacter sulfurreducens* was able to efficiently convert the  
19           acetate present in synthetic waste water into electric current ( $j=0.32 \text{ mA cm}^{-2}$ ) able to  
20           desalinate water. Moreover, we implemented an efficient start-up protocol where  
21           desalination up to 90 % occurred in a desalination cycle (water production:  $0.308 \text{ L m}^{-2}$   
22            $\text{h}^{-1}$ , initial salinity:  $9 \text{ mS cm}^{-1}$ , final salinity:  $<1 \text{ mS cm}^{-1}$ ) using a filter press-based  
23           MDC prototype without any energy supply (excluding peristaltic pump energy). This  
24           start-up protocol is not only optimized for time but also simplifies operational  
25           procedures making it a more feasible strategy for future scaling-up of MDCs either as a  
26           single process or as a pre-treatment method combined with other well established  
27           desalination technologies such as reverse osmosis (RO) or reverse electro dialysis.

29 **Introduction**

30 Shortage of fresh water is one of the major challenges for societies all over the world. In  
31 this sense, current water desalination technologies can significantly increase water  
32 resources for human consumption, industrial use and irrigation, but require significant  
33 electric or thermal energy. On top of the environmental impact due to brine disposal [1],  
34 reverse osmosis (RO) consumes around  $3.5 \text{ kWhm}^{-3}$  of electric energy [2] for seawater  
35 desalination with only a recovery of 50%, while thermal technologies could reach more  
36 than  $7 \text{ kWhm}^{-3}$  to drive desalination processes. The installed capacity of systems in year  
37 2015 was about  $86.8 \text{ million m}^3 \text{ day}^{-1}$  of desalted water, this is expected to increase  
38 drastically in the next years. The desalination market is mostly dominated by reverse  
39 osmosis (RO), compared to competition between multi-stage flash (MSF) and multi-  
40 effect distillation (MED). These systems require electric or thermal energy to drive the  
41 desalination process, and the equivalent amount of fossils fuel to produce the energy  
42 related to desalination processes (i.e.  $86.8 \text{ million m}^3 \text{ day}^{-1}$ ) is around 793 million tons  
43 per year, according to Kalogirou [3]. Thus, if desalination is accomplished by such  
44 technologies, environmental pollution would be a major concern because of green-  
45 house gases emissions. On top of that, conventional desalination technologies spend an  
46 important amount of energy to produce desalted water, so innovative desalination  
47 systems are required to be developed.

48  
49 Microbial Electrochemical Technologies (METs) constitute a platform [4] of emerging  
50 technologies based on the interaction between electroactive bacteria and electrodes.  
51 Indeed, a variant of the fuel cell, the microbial fuel cell (MFC), allows the direct  
52 transformation of soluble organic matter into electric current [5]. The produced power  
53 (in the range of  $0.001\text{-}19 \text{ W m}^{-2}$  (referenced to cross section) [6]) could be used in the  
54 same system to enhance organic matter degradation or drive other processes requiring

55 electrochemical energy, and operate in a self-sufficient and decentralised fashion as a  
56 passive system.

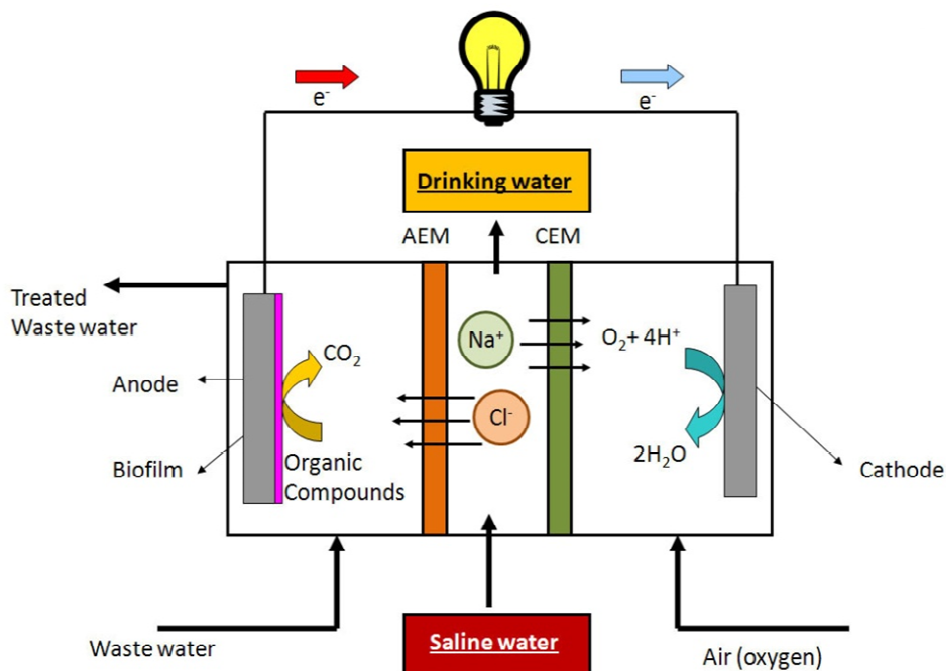
57

58 In this microbial electrochemical context, the Microbial Desalination Cell (MDC) is the  
59 integration of a MFC and an electrodialysis (ED) cell in order to treat wastewater and  
60 desalinate seawater. By using the energy provided by the oxidation of organic matter,  
61 contained in the wastewater, this system drives the migration of ions and the  
62 desalination process. Thus, MDC technology is able to desalinate saline water without  
63 consuming electric or thermal energy and allowing the use of the energy for any other  
64 processes. In this sense, MDC technology could be employed to save energy and avoid  
65 the greenhouse gases related to the conventional processes (seawater RO produces 1.78  
66 kg of CO<sub>2</sub> per m<sup>3</sup> using 600 g CO<sub>2</sub> kWh<sup>-1</sup> in the average European Union (EU) energy  
67 mix). Indeed, the versatile and simultaneous applications of MDC have made it a real  
68 and feasible alternative for both desalination and wastewater treatment [7].

69 The MDC unit is composed of at least three chambers (figure 1): 1) an anaerobic anodic  
70 chamber that contains the electroactive microbial community which first oxidises the  
71 organic matter (fuel) contained in wastewater and then transfer electrons to the anode;  
72 2) a central desalination compartment separated from the others by an anion exchange  
73 membrane (AEM) and a cation exchange membrane (CEM); 3) a cathodic chamber  
74 where the reduction counter-reaction occurs. In a MDC reactor, CEM and AEM are  
75 alternatively placed between the cathodic and the anodic compartment, as indicated in  
76 Figure 1. Moreover, an external load is placed between anode and cathode collector,  
77 allowing the flow of electric current. If organic matter is used to feed the anodic  
78 compartment, and the cathodic compartment is fed with a catholyte (for example, Fe<sup>3+</sup>  
79 or oxygen in acidic solution), then a potential difference is established between both  
80 electrodes. Due to the differential charges of the two chambers, anions and cations

81 migrate through the respective membranes raising the salt concentration in the anodic  
 82 and cathodic compartments while decreasing it in the saline compartment (central  
 83 compartment). Thus, the MDC constitutes a sustainable process since it does not require  
 84 external energy input because microbes harvest it from waste.

85 Different MDC designs have been reported in the literature from the first proof-of-  
 86 concept study [7,8], including cubic and tubular reactors [9-12], stacked cells [13, 14],  
 87 using batch recirculation [15, 16], biocathodes MDCs [17], increasing water production  
 88 by applying external voltage [18], or integrating innovative membranes (Forward  
 89 Osmosis) [19, 20] or ion exchange resins in the compartments [21]. Although most of  
 90 the MDC prototypes studied in the literature are lab scale (i.e. millilitres), a 100 L pilot  
 91 scale MDC unit achieving partial desalination of seawater has been reported [22]. Thus,  
 92 MDC technology has been proposed as a suitable pre-treatment for Reverse Osmosis to  
 93 reduce energy costs for desalination [23].



94  
 95 **Figure 1.** Diagram of MDC unit.  
 96

97 Regarding the performance of the MDC, the main limitations are i) the drastic increase  
98 of the internal resistance due to the changes in the conductivity of the medium, and the  
99 pH variations in the anodic chamber that can affect the biofilm growth. Related to the  
100 efficiency of the desalination process, the main constrains are limited potential to drive  
101 ion migration and back diffusion of salts between anodic/cathodic and saline  
102 compartment. For the application of MDC technology at a pilot scale, most of the  
103 studies use the same start-up protocol: a pre-adaptation of the biological anode under a  
104 MFC configuration [7,8], followed by the conversion of MFC into a MDC device by  
105 adding a supplementary chamber (saline compartment) that requires the disassembly of  
106 the whole system. This strategy for starting-up MDC is a time-consuming procedure of  
107 up to 20 days [24] and it does not favour reproducible experimental results at lab scale.  
108 Furthermore, most previous studies were conducted on millilitre-scale MDCs (<300 ml)  
109 where, to the best of our knowledge, just a few works reported on MDC over one litre  
110 [11,25]. So, using a more rationale start-up protocol could enable the scale-up of MDC  
111 technology in a realistic way and could help to improve the study of such systems by  
112 increasing reproducibility and avoiding time-consuming pre-acclimation strategies.

113

114 In the current work, we propose a rational and efficient start-up protocol where  
115 desalination up to 90% occurs from the first cycle under the final structural  
116 configuration. Once the protocol is performed, the system operates as an autonomous  
117 MDC without any energy supply (excluding peristaltic pump energy) and could be used  
118 at lab scale for systematic study of MDC performance under different experimental  
119 conditions.

120

121

## 122 **2. Experimental Section**

### 123 **2.1 Bacterial strain, culture condition.**

124 A pure culture of *Geobacter sulfurreducens* strain DL1 was used as inoculum for the  
125 MDC start-up protocol. The culture was routinely grown at 30 °C in septum-sealed  
126 serum bottles containing freshwater medium (FWM, pH=6.9, EC=12.4 mS cm<sup>-1</sup>) with  
127 the following mineral salts: NaHCO<sub>3</sub> 2.5 g L<sup>-1</sup>; NH<sub>4</sub>Cl 0.25 g L<sup>-1</sup>; NaH<sub>2</sub>PO<sub>4</sub>H<sub>2</sub>O 0.06 g  
128 L<sup>-1</sup>; KCl 0.1 g L<sup>-1</sup>; Fe(NH<sub>4</sub>)<sub>2</sub>(SO<sub>4</sub>)<sub>2</sub>6H<sub>2</sub>O 0.04 g L<sup>-1</sup>. The medium was supplemented  
129 with a trace mineral and vitamin solutions [26]. Sodium acetate (NaC<sub>2</sub>H<sub>3</sub>O<sub>2</sub> 1.64 g L<sup>-1</sup>  
130 or 20 mM) was used as electron donor and fumarate (C<sub>4</sub>H<sub>2</sub>Na<sub>2</sub>O<sub>4</sub>, 6.40 g L<sup>-1</sup> or 40 mM)  
131 as sole electron acceptor. Anaerobic conditions and pH buffering (pH 6.8-7.0) were  
132 assured by flushing a mixture of N<sub>2</sub>/CO<sub>2</sub> (80:20, industrial ALIGAL-12) into the culture  
133 media. Traces of oxygen were removed from the gas phase by passing the gas through  
134 heated copper fillings. Exponential-phase culture was used for the inoculation into the  
135 anode compartment.

136

### 137 **2.2 Microbial Desalination Cell device (MDC)**

138 A commercial multipurpose electrochemical reactor manufactured by ElectroCELL  
139 company (Electro MP-1, effective projected electrode area 100 cm<sup>2</sup>) was used as MDC  
140 device. The MDC prototype (see Supplementary Information, Figure S1) had a compact  
141 stack design consisting on several polypropylene compartments and neoprene gaskets  
142 for an optimal hermetically seal. The dynamic design of the device allows different cell  
143 configurations. In this case, the three compartment configuration was used. A  
144 desalination chamber (compartment volume: 70 cm<sup>3</sup>) separated the anodic and cathodic  
145 chambers (compartment volume of each one: 70 cm<sup>3</sup>) by an anionic exchange  
146 membrane (AMX Neosepta) and cation exchange membrane (CMX Neosepta),

147 respectively. Both electrodes (i.e. anode and cathode), were composed of carbon felt  
148 RVG 4000 (MERSEN Ltd.) and contained graphite plates as electric collectors. The  
149 device was closed with stainless steel screws in order to avoid any leakage of the  
150 system.

151 The three tanks were connected to the MDC prototype by Pharmed Tubing with an  
152 internal diameter 1/4" (SAINT-GOBAIN). A four-channel peristaltic pump (Heidolph  
153 Pumpdrive 5201) was used for the recirculation of the streams through the system.  
154 Figure S2 (see Supplementary Information) shows a flow diagram of the MDC  
155 experimental set-up.

156 The flow rate of all solutions was of 75 mL min<sup>-1</sup>. The whole system was placed in a  
157 temperature controlled room at 30 °C and kept under anaerobic conditions by flushing a  
158 mixture of N<sub>2</sub>/CO<sub>2</sub> (80:20, industrial ALIGAL-12) into the tanks. Two reference  
159 electrodes (Ag/AgCl KCl 3.5 M, CRISON) were placed into the cell, one in the  
160 geometric center of the anodic compartment and the other in the cathodic compartment,  
161 in order to measure anode and cathode potential respectively. A power supply (Aim-  
162 TTi, 0-15 V, 0-5 A) was connected to the electrochemical reactor to be used during  
163 start-up protocol (see Supplementary Information, Figure S1 and S2).

164

## 165 **2.3. Start-up and operation procedure**

### 166 **2.3.1 MDC configuration testing**

167 A preliminary process of conventional electro dialysis under abiotic conditions was  
168 performed in order to test if the prototype's configuration was feasible for desalination  
169 operation. A 2 L solution of FWM supplemented with 20 mM of acetate (1.64 g L<sup>-1</sup>  
170 sodium acetate) as sole electron donor was used as anolyte and a 3.55 g L<sup>-1</sup> Na<sub>2</sub>SO<sub>4</sub>  
171 solution as catholyte (25 mM Na<sub>2</sub>SO<sub>4</sub>). A power supply applied a cell potential of 3 V

172 between anode (positive terminal) and cathode (negative terminal). The saline stream  
173 consisted on 2 L of 5 g L<sup>-1</sup> NaHCO<sub>3</sub> (pH=8.70, CE=5.1 mS cm<sup>-1</sup>). The system was  
174 operated in batch mode (streams recirculation) with a multichannel peristaltic pump  
175 with flow rate 75 mL min<sup>-1</sup> for all the streams (anolyte, catholyte and saline solution).

176

### 177 **2.3.2 Start-up procedure**

178 Prior to inoculation, the cell was sterilized by the recirculation of 70% w/w  
179 ethanol/water solution through the whole system (prototype and tubing). A filtered gas  
180 mixture of N<sub>2</sub>/CO<sub>2</sub> was gassed through MDC for 2 hours in order to guarantee ethanol  
181 evaporation and an anoxic environment inside the device. Also, electrolytes and saline  
182 solutions were degassed. The anolyte was made of 2 L of FWM with 1.64 g L<sup>-1</sup> sodium  
183 acetate (without any terminal electron acceptor, 20 mM, pH=6.95, CE=5.95 mS cm<sup>-1</sup>),  
184 and the catholyte was 2 L of 3.55 g L<sup>-1</sup> Na<sub>2</sub>SO<sub>4</sub> (0.0025 mM, pH=7.87, CE=4.74 mS  
185 cm<sup>-1</sup>) solution. The saline solution was 2 L of 1.25 g L<sup>-1</sup> sodium bicarbonate (15 mM ,  
186 pH=8.70, CE=5.1 mS cm<sup>-1</sup>).

187 It is important to note that the main role of using sodium bicarbonate solution as saline  
188 stream in this step is to avoid pH and/or conductivity changes in anodic media from  
189 continuous migration of anions (i.e. HCO<sub>3</sub><sup>-</sup>) from saline compartment, thus preserving  
190 optimum anode environment for biofilm colonization of the anode surface.

191 The volume relation of the electrolytes and saline solution was of 1:1:1 (V<sub>an.</sub>:V<sub>cat</sub> :  
192 V<sub>desal</sub>). The cell potential was fixed at 1.0 V (i.e. potential between anode and cathode)  
193 and then all three solutions were recirculated through the system overnight prior to  
194 anode inoculation in order to remove any dead volumes or stagnant zones in the system.  
195 After this, pump recirculation is switched off. Then, the anodic chamber was inoculated  
196 with 300 ml of exponential-phase *Geobacter sulfurreducens* culture. After inoculation,



197 the system was allowed to incubate overnight, to ensure cells adhesion to the anode.  
198 After incubation, the pumps were activated to recirculate the different solutions through  
199 the system. The cell potential (i.e. 1.0 V) is maintained until anode potential and current  
200 density are almost constant (45 hours approx., see figure 4A). After this, the cell  
201 potential is increased to 1.5V to allow growth of biofilm on anode surface (70 hours  
202 approx.). This first cycle was part of the start-up protocol and involved sodium  
203 bicarbonate desalination, in a MEC configuration, since a cell potential of 1.0-1.5 V was  
204 applied using an external power supply.

205

### 206 **2.3.3 Desalination operation**

207 Once the start-up protocol was performed, NaCl desalination was carried out in the  
208 MDC. The peristaltic pump was deactivated and the power supply was disconnected  
209 from electrode collectors. Then, MDC electrode collectors were connected to an  
210 external load of 2.5  $\Omega$ . This value of the external load was selected to ensure proper  
211 measurement of the electric current in the system by voltage drop measurement.  
212 Moreover, it is important to note that in the present study the MDC operates near short  
213 circuit (low external resistance value) in order to provide all the energy from organic  
214 matter oxidation to the desalination process, as the main objective is to maximize the  
215 water production. Anolyte tank was refreshed with new solution of the same  
216 composition and volume as above. The catholyte was replaced with 2 L of 3 g L<sup>-1</sup>  
217 NaClO solution (0.3 %, pH=11.14, CE=14.57 mS cm<sup>-1</sup>). The saline solution was  
218 replaced by 0.2 L of 5 g L<sup>-1</sup> NaCl. The volume relation was 10:10:1 ( $V_{an}:V_{cat}:V_{desal}$ ).  
219 Once all the solutions were replaced, the recirculation pump was activated to start  
220 desalination.

221

222 **2.4 Electrochemical equipment**

223 The data acquisition of the anode/cathode potential and electric current was performed  
224 using a custom Visual Basic Program and ModBus modules (ICP-DAS). Reference  
225 electrodes (Ag/AgCl 3.5 M, CRISON) were placed in anode and cathode compartment,  
226 using lugging capillary (Teflon).

227

228 **2.5 Analytical methods**

229 Electric conductivity measurements were carried out using GLP 31 conductivity meter  
230 (CRISON). A GLP 21 pH-meter (CRISON) was used to measure pH. Both  
231 measurements were recorded at 25 °C. For conductivity readings, solution samples were  
232 analyzed throughout the experiments. Carrying out a set of conductivity calibration tests  
233 at  $25.0 \pm 0.4$  °C, determined a conversion factor of  $\kappa = 0.55$  for converting electric  
234 conductivity (EC,  $\text{mS cm}^{-1}$ ) into NaCl concentration ( $\text{g L}^{-1}$ ) (see Supplementary  
235 Information).

236 For total COD determination, 15 mL of sample were collected and kept at 4°C until  
237 analysis by APHA method 5520. The content of acetate in the anolyte was measured  
238 with HPLC with a ZORBAX PL Hi-Plex H Guard Column (50 mm  $\times$  7.7 mm, Agilent  
239 Technologies, Madrid, Spain) and mobile phase of 0.1%  $\text{H}_3\text{PO}_4$ . The sample volume  
240 was 50  $\mu\text{L}$ , mobilized at a flow rate of  $0.5 \text{ mL} \cdot \text{min}^{-1}$ . Acetate was detected by using UV  
241 detector at 210 nm.

242

243 **2.6 Process parameters**

244 Current density ( $j$ ,  $\text{mA cm}^{-2}$ ), and power ( $P$ ,  $W$ ) in all experiments were calculated using  
245 Eqs. 1, and 2, respectively.

246 
$$j = \frac{I}{A_m} \tag{1}$$

247  $P = E_{cell} \times I$  (2)

248 where  $E_{cell}$  is the voltage applied across the MDC system (V),  $I$  is the operating current  
 249 (A) and  $A_m$  is the effective electrode surface area (cm<sup>2</sup>). Cell potential, anode and  
 250 cathode potential, as well as electric current data were measured throughout the process.  
 251 Specific energy consumption (SEC, kWh m<sup>-3</sup>) defines the energy required for producing  
 252 one cubic meter of fresh drinking water by the MDC system (Eq. 3).

253  $SEC = \frac{1}{3.6 \times 10^6 \times Q_t} \int E_{cell} I(t) dt$  (3)

254 In Eq. 3,  $Q_t$  is the volume of the treated water (m<sup>3</sup>). In desalination experiments, water  
 255 production ( $WP$ , m<sup>3</sup> m<sup>-2</sup>h), defining the cubic meter of drinking water produced by the  
 256 MDC system per available membrane surface area per hour, was calculated using Eq. 4;

257  $WP = \frac{Q_t}{A_m \times t_d}$  (4)

258 where,  $t_d$  is the total time taken for the completion of the desalination process (h).  
 259 Current efficiency ( $\eta_c$ , %) defines the ratio of total mass of salt removed from the saline  
 260 channel to the amount of electric charge transferred across the membranes (ECT, C m<sup>-3</sup>)  
 261 over a complete process of desalination.  $\eta_c$  and ECT were calculated using Eqs. 5 and 6,  
 262 respectively.

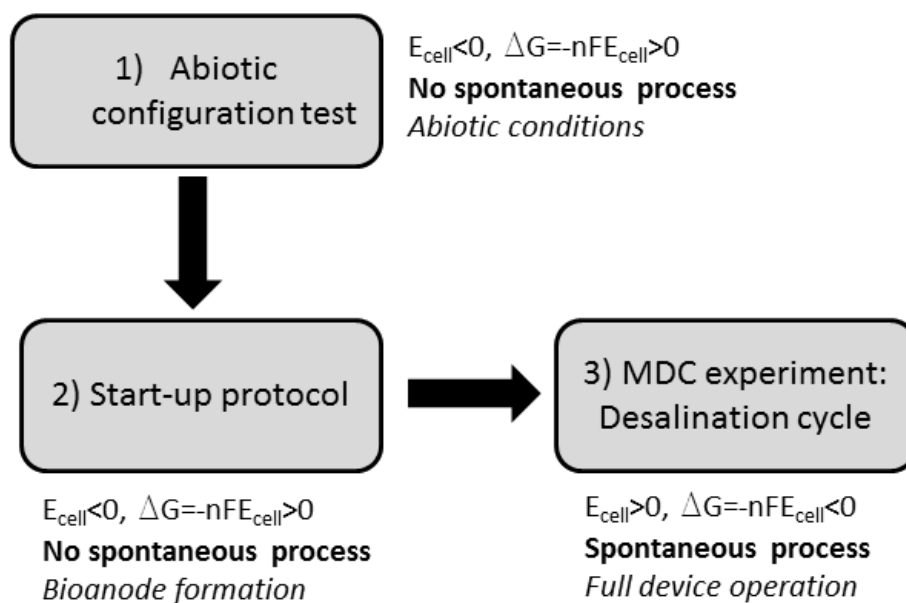
263  $\eta_c = \frac{v \times z \times F \times (c_s^f - c_s^p)}{ECT}$  (5)

264  $ECT = \frac{1}{Q} \int I(t) dt$  (6)

265 where,  $v$  and  $z$  represent the stoichiometric coefficient and the valence of the salt ions,  
 266 respectively and  $F$  is the Faraday constant (96,485 C mol<sup>-1</sup>).  $c_s^f$  and  $c_s^p$  represent the  
 267 initial and final molar concentrations of salt in the saline tank (mol m<sup>-3</sup>), respectively.  
 268

### 269 3. Results and Discussion

270 In this section we have explored a rational and efficient start-up protocol where  
 271 desalination occurs (Figure 2) while current efficiency was compared to conventional  
 272 electro dialysis.



273

274 **Figure 2.** Schematic diagram: start-up protocol for MDC study at lab scale.

275 **3.1 Testing desalination under an abiotic MDC configuration**

276 In order to characterize the performance of the cell stack under non-limiting conditions  
 277 an abiotic electrochemical desalination was carried out. An electric potential of 3.0 V  
 278 was applied between anode (positive terminal) and cathode (negative terminal). Under  
 279 this condition, water was oxidised on the anode ( $2\text{H}_2\text{O} (\text{l}) \rightarrow \text{O}_2 (\text{g}) + 4\text{H}^+ + 4\text{e}^-$ ,  $E^0 = -$   
 280 1.23 V) while water was reduced on the cathode ( $4\text{H}_2\text{O} (\text{l}) + 4\text{e}^- \rightarrow 2\text{H}_2 (\text{g}) + 4\text{OH}^-$ ,  $E^0 =$   
 281  $-0.42 \text{ V}$ ) and a solution of  $5 \text{ g L}^{-1} \text{ NaHCO}_3$  was desalinated in the middle compartment  
 282 (Figure 3C).

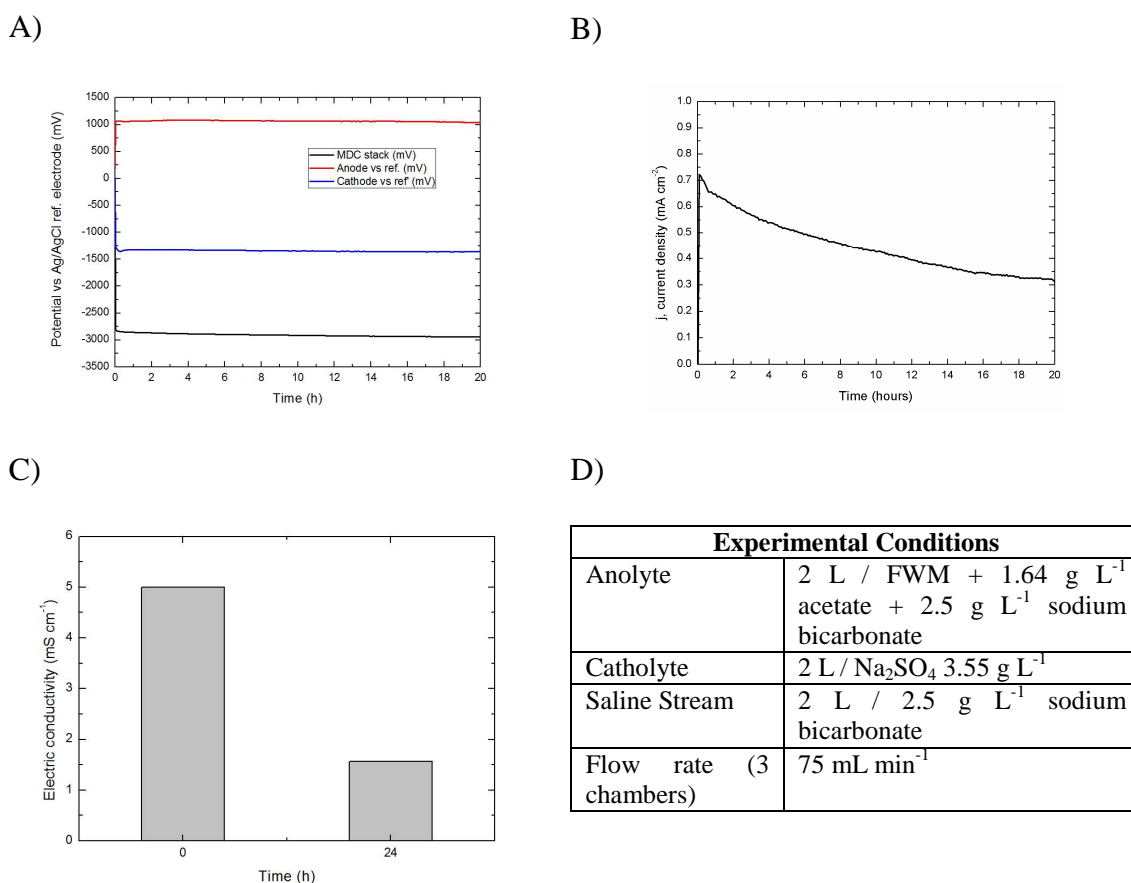
283 The electrodes potential remained constant throughout the desalination process  
 284 (Figure 3A). It is known that the potential of the whole MDC should correspond to the  
 285 following equation:

286  $E_{\text{cell}} = E_{\text{cathode}} - E_{\text{anode}} - R_{\text{cell}} I$  [Ecell < 0, ΔG = -nFEcell > 0, No spontaneous process]

287 (7)

288 where  $E_{\text{cell}}$  is the applied potential (mV),  $E_{\text{cathode}}$  is the cathode potential (mV),  $E_{\text{anode}}$  is  
 289 the anode potential (mV),  $R_{\text{cell}}$  is the overall resistance of the cell ( $\Omega$ ), and  $I$  is the

290 electric current that circulates through the system (mA). The electric current started at a  
 291 maximum current density of  $j = 0.72 \text{ mA cm}^{-2}$  and decreased to values around  $0.32 \text{ mA}$   
 292  $\text{cm}^{-2}$  after 20 hours of polarization (figure 3B). This behaviour of the current output is  
 293 typical of conventional electro dialysis systems [27] operating at a constant applied  
 294 potential in batch mode. This is due to the electric conductivity of the saline  
 295 compartment (i.e. saline stream) decreasing during the desalination process, and in turn  
 296 increasing the overall resistance of the cell. Indeed, after 24 hours of cell operation, a  
 297 68.6% desalination was correlated to a 75% decrease of the electric current (Figure 3C).



298 **Figure 3.** A) Potential for the anode, the cathode and the whole cell; B) Electric current  
 299 produced during the desalination process; C) Electric conductivity drop in the  
 300 desalination compartment; D) Chemical composition of anolyte, catholyte and saline  
 301 stream employed in the MDC configuration test.

302

303 In this abiotic experiment desalination process was completed after 24 h, thus specific  
304 energy consumption (SEC) was 1.46 kWh m<sup>-3</sup>, water production (WP) 10 L m<sup>-2</sup> h (0.01  
305 m<sup>3</sup> m<sup>-2</sup> h) for the initial conductivity of 5 mS cm<sup>-1</sup> (i.e. brackish water), and the current  
306 efficiency of the process was  $\eta_c=94\%$ . For similar water conditions in electro dialysis  
307 experiments (analogous ion exchange membranes system), the SEC is in the range of  
308 0.6-0.8 kWh m<sup>-3</sup> [27]. Even if the systems are not comparable from construction point  
309 of view (i.e. different configuration of the unit cell, higher thickness for anode/cathode  
310 and saline compartments, low conductivity in the anode compartment to avoid  
311 microorganisms saline stress), abiotic desalination experiments could be useful to  
312 compare the energy consumption in different MDC prototypes at lab scale. Also, it is  
313 important to note that efficiency in the desalination process is similar to conventional  
314 electro dialysis stacks, suggesting proper assembly and a correct operation in abiotic  
315 conditions for the MDC system. The current efficiency is lower than 100%, due to the  
316 non-ideal membranes and the existence of shunt currents.

317

### 318 **3.2 Start-up procedure for the Microbial Desalination Cell (MDC).**

319 Once the system was abiotically tested, the MDC was ready to host a microbial anode.  
320 So, maintaining the previous setup and electrolytes composition, a cell potential of 1.0  
321 V was set between electrodes and sterile solutions were recirculated overnight through  
322 the two chambers. The anode was inoculated without recirculation (recirculation pump  
323 switched OFF) and incubated for 20 hours, as previously noted in section 2.3.2. So, the  
324 complete acetate oxidation to CO<sub>2</sub> by *G.sulfurreducens* ( $C_2H_4O_2 + 2 H_2O \rightarrow 2 CO_2 + 8$   
325  $e^- + 8 H^+$ ,  $E^\circ=-0.290$  V) and the reduction of water ( $2 H_2O + 2e^- \rightarrow H_2 + 2 OH^-$ ,  $E^\circ=-$   
326  $0.8277$  V) were the main reactions on anode and cathode respectively, being the process  
327 non-spontaneous ( $E_{cell}<0$ ,  $\Delta G=-nFE_{cell}>0$ ).

328 During this period (Figure 4A) the anode potential dropped from 500 mV to values near  
329 -300 mV (vs. Ag/AgCl KCl 3.5 M) while the current density increased from the original  
330 values to  $j=0.048 \text{ mA cm}^{-2}$ . Both phenomena are characteristic of *G. sulfurreducens*  
331 electroactive behaviour [28–30] when the electric current is obtained from acetate  
332 oxidation. On the other hand, the cathode potential decreased following the anode  
333 potential in order to maintain cell potential (water reduction was the main reaction in  
334 the cathode).

335 After 20 hours of operation, the electric current decreased 33% (Figure 4B). Local  
336 starvation of electron donors (i.e. acetate) as a consequence of an insufficient mixing of  
337 the solution may have caused this bacterial metabolic limitation. Moreover, local pH  
338 decrease could also be a factor that affects bacterial cells performance. Even if  
339 bicarbonate ions migrate from the desalinization chamber, the lack of flow through the  
340 anode chamber could produce internal biofilm acidification as a result of microbial  
341 metabolism. Those physiological limitations were confirmed once electrolyte  
342 recirculation was re-started according to the sudden raise of 375% in current generation  
343 (Figure 4B).

344 After 24 hours operating with continuous media flow, a stable current output of 11.2 mA  
345 was reached ( $j=0.112 \text{ mA cm}^{-2}$ ). At the same time, the anode potential decreased  
346 indicating an insufficient anode polarization. This is consistent with the maximal  
347 electroactive performance of *G. sulfurreducens* (-0.2 V (vs. Ag/AgCl) reported  
348 elsewhere [31,32]. When the electrode polarization was below this potential, the biofilm  
349 cells became reduced due to the charge accumulation in a network of redox proteins  
350 made of multiheme c-type cytochromes [30,33,34]. The outstanding nature of this  
351 network allows *Geobacter* strains to exhibit a capacitive property unique in microbes  
352 [35,36]. So, in order to increase current production and biofilm discharge, cell voltage

353 was extended from 1 V to 1.5 V, leading to the expected rise in current output of 330%  
354 (i.e. from 9.6 to 32.0 mA) in just 8 h. Moreover, upon repolarization after inoculation,  
355 there was a discharge peak confirming a charge accumulation in the cytochrome  
356 network due to the capacitor effect of the biofilm. Then, current increased from 24.0 to  
357 32.0 mA suggesting the presence of a biofilm colonizing the electrode surface with  
358 enough electroactive capacity to produce an electric field in the system able to drive the  
359 migration of ions from the saline compartments to anode/cathode compartments.  
360 Indeed, electric conductivity of the saline chamber significantly decreased until it had  
361 removed 94% of the initial bicarbonate ion at the end of the desalination cycle (110 h)  
362 (Figure 4C).

363 It is important to note that the main role of using sodium bicarbonate solution as saline  
364 stream is to avoid pH and/or conductivity changes in anodic media from continuous  
365 migration of anions (i.e.  $\text{HCO}_3^-$ ) from saline compartment, thus preserving optimum  
366 anode environment for biofilm colonization of the anode surface. In this sense, also  
367 other experimental conditions as high solution flow rate ( $75 \text{ mL min}^{-1}$ ) ensured adequate  
368 substrate concentration inside the carbon felt anode, minimizing local pH variations  
369 (Figure S3) or substrate depletion (removal of COD < 49% of the original COD during  
370 the start-up procedure).

371

372

373

374

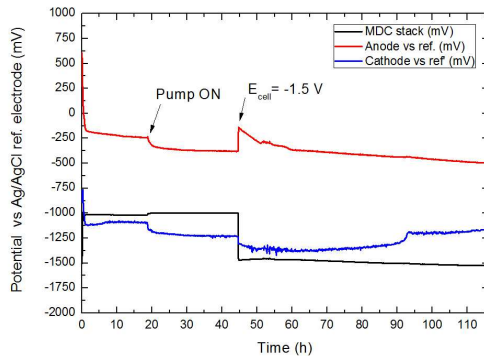
375

376

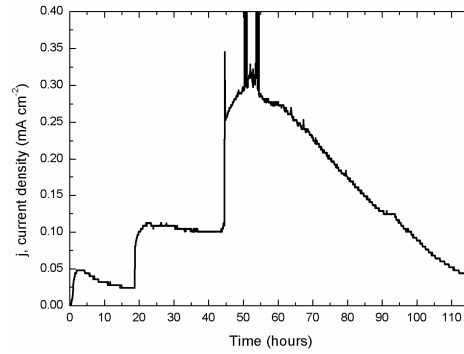
377



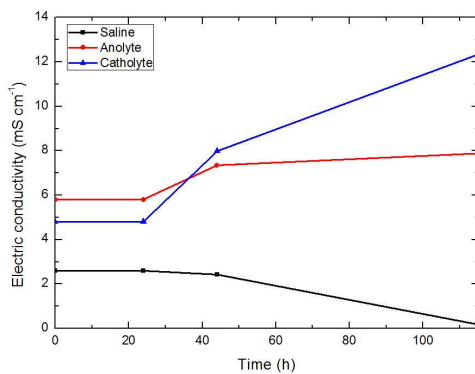
A)



B)



C)



D)

Experimental Conditions	
Anolyte	2 L / FWM + 1.64 g L <sup>-1</sup> acetate + 2.5 g L <sup>-1</sup> sodium bicarbonate
Catholyte	2 L / Na <sub>2</sub> SO <sub>4</sub> 3.55 g L <sup>-1</sup>
Saline Stream	2 L / 1.25 g L <sup>-1</sup> sodium bicarbonate
Flow rate (3 chambers)	75 mL min <sup>-1</sup>

378 **Figure 4.** A) Potential for anode, cathode and whole cell. Black arrow indicate time for  
 379 starting up the recirculation; B) Electric current obtained during the desalination  
 380 process; C) Electric conductivity in the three chambers (anodic, cathodic and saline  
 381 chamber) D) Characteristics of anolyte, catholyte and saline solution used during the  
 382 MDC start-up procedure.

383

### 384 3.3 Microbial Desalination Process

385 The start-up period was considered to be completed after 100 hours of operation, when  
 386 an electroactive *G.sulfurreducens* biofilm had developed. At this point, the catholyte  
 387 was replaced with 2 L of NaClO 3 g L<sup>-1</sup> (0.3%, pH=12), the anolyte was refreshed (2 L,  
 388 FWM, pH=6.9, 1.64 g L<sup>-1</sup> / 20 mM sodium acetate) and saline solution was changed to  
 389 0.2 L solution of NaCl 5g L<sup>-1</sup>. Finally, the circuit was closed using a shunt resistance

390 (external load) of 2.5  $\Omega$  that allowed monitoring of the electric current through the  
391 MDC unit. In this condition, the oxidation of acetate to CO<sub>2</sub> by *G.sulfurreducens* and  
392 the reduction of NaClO to chloride ion ( $\text{ClO}^- + \text{H}_2\text{O} + 2 \text{e}^- \longrightarrow \text{Cl}^- + 2 \text{OH}^-$ ,  $E^\circ=0.89$   
393 V) are the main reactions on anode and cathode respectively, enabling the spontaneous  
394 process of desalination (migration of ions from saline compartment,  $E_{\text{cell}}=E_{\text{cathode}}-$   
395  $E_{\text{anode}}>0$ ,  $\Delta G=-nFE_{\text{cell}}<0$ ).

396 During the initial desalination period, the electric current production dropped from 28  
397 mA to 15 mA while the anode potential remained stable (Figure 5A). The reduction of  
398 electric conductivity of the saline stream –and the increased internal resistance due to  
399 this fact - is the main reason for this current shift. Although more than 20% of the total  
400 acetate (enough for microbial growth) was detected in the anolyte after this current  
401 drop, anolyte was replaced by new fresh anolyte (2 L, FWM, 1.64 g L<sup>-1</sup> / 20 mM  
402 sodium acetate) in order to assure bioanode performance (i.e. no influence by changes  
403 concentration or metabolite accumulation). In the same context, catholyte was also  
404 replaced by new media (2 L, NaClO 3 g L<sup>-1</sup>, pH=12).

405 The MDC device was able to desalinate 65% of the NaCl content in the first 18 hours,  
406 and 90% in 65 hours (end of desalination cycle, 1mS cm<sup>-1</sup>, drinking water limit) (Figure  
407 5C). At the same time, both the anolyte and the catholyte conductivity remained stable,  
408 mainly due to the high ratio anolyte/saline volume and/or catholyte/saline volume.  
409 Electric resistance of MDC system was constant (2.5  $\Omega$ , value of external load).

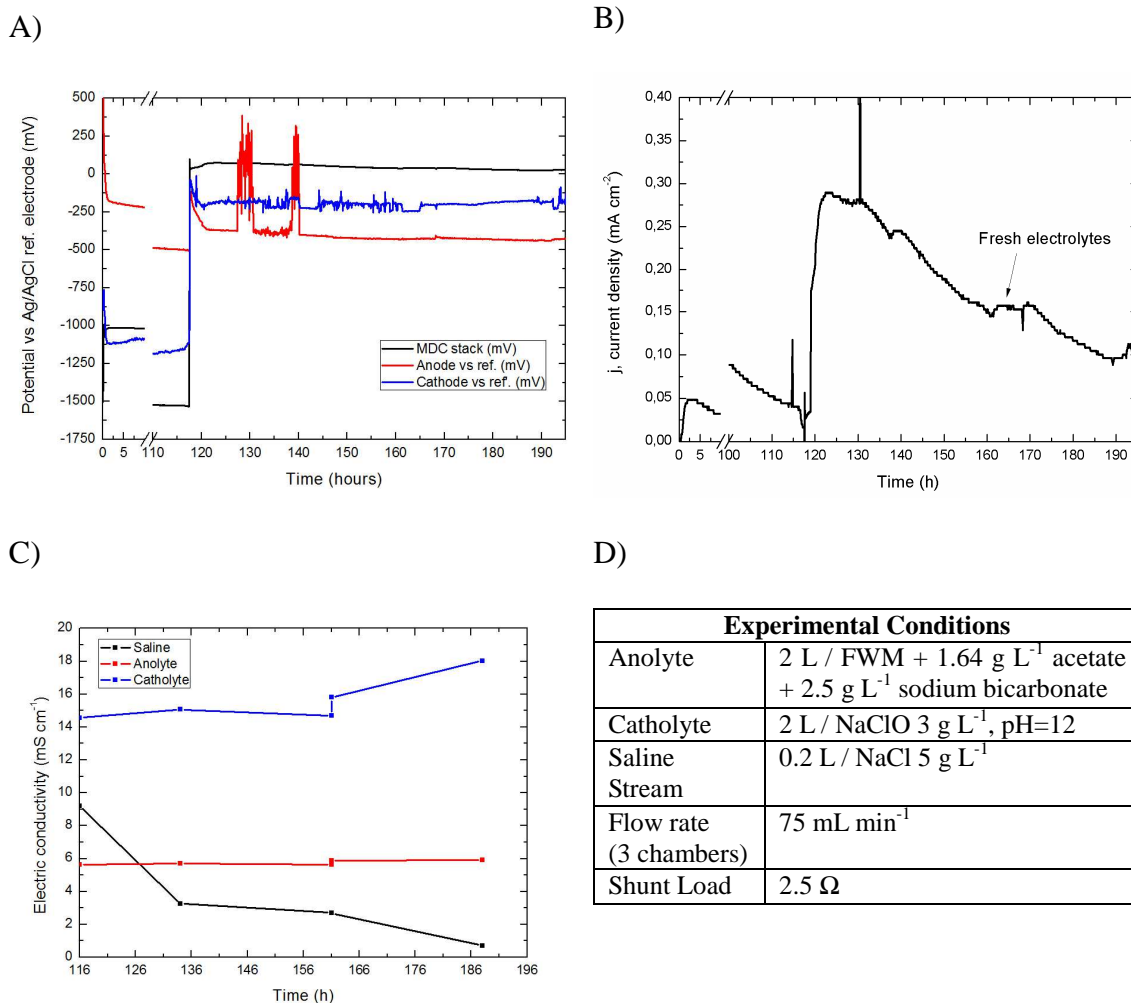
410

411

412

413

414



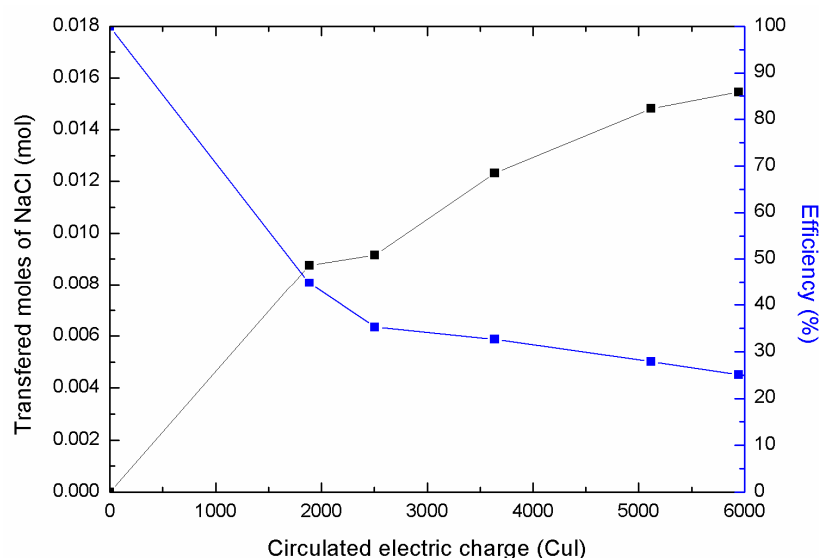
415 **Figure 5.** A) Potential for anode, cathode and whole cell; B) Electric current produced  
 416 during the desalination process. Black arrow indicates the replacement of anolyte and  
 417 catholyte; C) Electric conductivity of the anodic, cathodic and saline streams; D)  
 418 Chemical composition for anolyte, catholyte and saline stream employed in the  
 419 desalination process  
 420 Another key aspect for the proper performance of the microbial biofilm on the anode is  
 421 the pH. In that sense, both anolyte and catholyte pH slightly increase in less than one  
 422 unit allowing the maintenance of the anodic biofilm (Figure S4). Actually, COD  
 423 removal was incremented from 49% under power supply conditions to 53% under MDC  
 424 mode operation.  
 425 At the end of the process, water production was 0.308 L m<sup>-2</sup> h (initial concentration

426 NaCl 5 g L<sup>-1</sup>) while efficiency vs circulated electric charge was  $\eta_c=25\%$  (Figure 6). The  
427 decrease of the efficiency could be attributed to back-diffusion processes [37] and the  
428 low available potential (compared to the abiotic desalination). Also, it is assumable that  
429 initial conductivity of saline stream and ratio among anolyte-catholyte-saline tank  
430 volumes would have and strong effect on the efficiency of the process, and this effect  
431 should be studied before scale-up and optimization of MDC technology.

432 In relation to the specific energy consumption (SEC), it is important to note that energy  
433 consumed associated to MDC-based desalination was equal to 0 (excluding pumping  
434 energy). We indeed considered negligible the energy produced by the external load used  
435 for voltage/current monitoring (i.e. energy produced 0.082 Wh, 412 Wh per m<sup>-3</sup> of  
436 desalted water, or 20.63 Wh per m<sup>-3</sup> of treated water),.

437 Conventional reverse osmosis system or electrodialysis system typically require an  
438 energy value of 0.5-0.8 kWh m<sup>-3</sup> to drive the same desalination process (from of 5 mS  
439 cm<sup>-1</sup> to 1 mS cm<sup>-1</sup>) exhibited by our MDC [38]. On top of that, the associated emissions  
440 of 0.3-0.48 kg m<sup>-3</sup> of CO<sub>2</sub> would be avoided (using the value 600 g CO<sub>2</sub> kWh<sup>-1</sup> in the  
441 average European Union energy mix [39]). Moreover, if we consider that the energy for  
442 waste water treatment is in the range of 0.2-0.4 kWh m<sup>-3</sup>, and assuming a ratio waste  
443 water/desalted water 10:1, we could avoid the emissions of 1.2-2.4 kg of CO<sub>2</sub> per m<sup>-3</sup> of  
444 desalted water. Thus, the challenge is to develop MDC technology and scale up to a  
445 reasonable production of desalinated water (i.e. small and medium size desalination  
446 plants are in the range of 2,000-10,000 m<sup>3</sup> day<sup>-1</sup>).

447



448

449 **Figure 6.** NaCl transferred (mol) and Efficiency (%) of the process vs circulated electric  
 450 charge (Cul).

451 The MDC system presented in this paper was able to produce desalinated water with a  
 452 simplified start-up procedure compared to other experimental systems reported in the  
 453 literature adapting the microorganism before starting the MDC operation [24,25], thus  
 454 significantly reducing the start-up period. Also, the start-up strategy presented in this  
 455 study avoids the need of pre-running as a MFC and disassembly for incorporating the  
 456 saline compartment, as presented in some papers for MDC operation at lab scale  
 457 [7,8,13]. So, the start-up protocol presented is not only optimized for time but also  
 458 simplified in operation, making it a more feasible strategy for future scaling-up. Also,  
 459 the start-up protocol presented could be used at lab scale to systematically study MDC  
 460 performance. It is useful tool to design and optimize MDC experimental set-ups (i.e.  
 461 study of energy consumption in abiotic conditions).

462 The desalination performances of several MDC studies (including the current one) are  
 463 shown in Table 1. Even the experimental set-ups presented in the literature are different  
 464 in configuration (i.e. compartments volumes, cathode reactions, operation mode in  
 465 continuous or batch) and it is not possible direct comparison among them, the efficiency

466 of our treatment was remarkable considering the low ratio of volumes for anolyte and  
467 catholyte compared to the ones reported in the literature with similar removal rate. In  
468 some cases, those volumes ratios were quadrupled or even 100 times larger than the  
469 volumes employed in our system [8,13]. Those studies using similar volume ratio  
470 reached less than 50% of the desalination obtained in the MDC presented in this study  
471 [9,40,41].

**Table 1.** MDC system comparison (<sup>a</sup> V<sub>an</sub>: anolyte volume, V<sub>cat</sub>: catholyte volume, V<sub>desal</sub>: desalinated water volume; <sup>b</sup> With additional voltage of 0.55 V; Removal (%): desalination percentage; COD: percentage of Chemical Oxygen Demand removal.

V <sub>an</sub> : V <sub>cat</sub> : V <sub>desal</sub> <sup>a</sup>	Start-up protocol	Initial concentration of Salt	Salt Removal (%)	COD Removal(%)	Ref.
100:33:1	Transfer of pre-adapted MFC anode (10 days)	5 g.l <sup>-1</sup> NaCl	88	-	[7]
36:11:1	Transfer of pre- adapted MFC anode (10 days)	20 g.l <sup>-1</sup> NaCl	80	-	[13]
10:10:1	Bicarbonate desalination	5 g.l <sup>-1</sup> NaCl	90	53	This study
4:4:1	1 week anode in-sit stabilization	0.5 g.l <sup>-1</sup> NaCl	95.8	-	[25]
4:2:1	Inoculation with a mixture sludge	35 g.l <sup>-1</sup> NaCl	42	74-77	[22]
3:3:1	Transfer of pre- adapted MFC anode	5 g.l <sup>-1</sup> NaCl	46	25	[24]
1.5:1.8:1	Transfer of pre- adapted MFC anode	20 g.l <sup>-1</sup> NaCl	<84	72-94	[8]
1:2:1	Inoculation of a pre-a adapted biofilm	5 g.l <sup>-1</sup> NaCl	43	-	[9]
1:2:1	40 days anode <i>in situ</i> stabilization	20 g.l <sup>-1</sup> NaCl	37 <sup>e,b</sup>	-	[40]

Related to volume ratios, in the present MDC system 10:10:1 ratio was key to avoid the generation of brine, one of the main environmental problems associated to desalination technologies. However, more research should be performed to optimize a) the ratios for different applications (i.e. desalination of brackish water for irrigation, seawater for drinking water) and b) the nature and organic load of the wastewater (i.e. municipal or industrial wastewater). Other important parameter to explore in order to maximize water production would be the thickness of the saline compartment that would decrease internal resistance of the MDC system [41].

From the point of view of energy production in MDC systems, an increase in the energy production is related to a drastic decrease in desalination rate or production of water, as a great amount of available energy from water oxidation is diverted towards energy production (rather than desalination process). Even whether the production of energy is an interesting topic itself, increasing desalinated water production is a key point to develop MDCs as sustainable and low-energy desalination technology. For this reason, in the present study the MDC operates near short circuit conditions, thus providing all the energy from organic matter oxidation to the desalination process, maximizing the water production.

It is important to note here that in the case of MDC, to operate in such conditions of low external load, it is not producing a degradation of the biofilm performance due to acidification of the media. The reason is that even the operation conditions are near the short circuit conditions from the point of view of the electrochemical device, the anode potential is similar to the equilibrium (i.e. open circuit potential) of the bioanode (see figure 5A, red line). So, short circuit condition for the MDC is somehow different from MFC short circuit conditions, as in the latter the anode potential is decreased due to high overpotential, thus providing higher density current (i.e. higher rate of organic



matter oxidation) and consequently problems of biofilm acidification, producing decrease in the performance of the system. In the case of MDC system, a part of the available electrochemical potential in the whole device is dropped in the saline compartment, and this effect is more noticeable when desalination process is progressing.

Finally, the use of NaClO reduction as the cathodic reaction (used in this study) has been tested in similar bioelectrochemical systems for waste water treatment [42] as a suitable alternative for oxygen reduction with increased performance (due to faster kinetics). So far, the present study is the first using a MDC with this cathodic reaction for desalination. However, it is important to indicate that the use of NaClO as catholyte could produce both damage on membrane surface in the long term and environmental issues related to chlorinated by-products formation (i.e. chlorinated organic matter). Consequently, more strategies for cathodic reactions and catholyte regeneration should be studied in the future to enable the development of MDC technology as sustainable desalination process, as well as operation with real waste water and brackish/sea water.

#### **4. Conclusions**

Microbial Desalination Cells constitute an innovative technology where microbial fuel cells and electrodialysis merge in the same device for obtaining fresh water from saline water with no energy-associated cost and greenhouse gas emissions. However, a number of factors should be further explored in order to optimized the methodology and make it profitable. The start-up procedure as well as the modular nature of our MDC prototype was demonstrated a viable alternative to the conventional procedures used. The start-up protocol presented here, could allow our MDC prototype to be a real possibility for scaling-up as either a stand-alone process or as a pre-treatment method combined with other well established desalination technologies such as reverse osmosis (RO) [9,23] or reverse electrodialysis.

## References

1. Elimelech, M.; Phillip, W. A. The Future of Seawater Desalination: Energy, Technology, and the Environment. *Science* **2011**, *333*, 712–717.
2. MacHarg, J.; Seacord, T. S.; Sessions, B. Affordable Desalination Collaboration (ADC) baseline tests reveal trends in membrane performance. *Desalination Water Reuse* **2008**, *18/2*.
3. Kalogirou, S.A., Seawater desalination using renewable energy sources, *Prog. Energ. Combust.* **2005**, *31*, Pages 242–281
4. Schröder, U.; Harnisch, F.; Angenent, L. T. Microbial electrochemistry and technology: terminology and classification. *Energy Env. Sci* **2015**, *8*, 513–519.
5. Borjas, Z.; Ortiz, J.M.; Aldaz, A.; Feliu, J.; Esteve-Núñez, A., Strategies for Reducing the Start-up Operation of Microbial Electrochemical Treatments of Urban Wastewater, *Energies* **2015**, *8*, 14064–14077.
6. Logan, B. E.; Wallack, M. J.; Kim, K.; He, W.; Feng, Y.; Saikaly, P.E., Assessment of Microbial Fuel Cell Configurations and Power Densities, *Environ. Sci. Technol. Lett.* **2015**, *2*, 206–214.
7. Cao, X.; Huang, X.; Liang, P.; Xiao, K.; Zhou, Y.; Zhang, X.; Logan, B. E. A New Method for Water Desalination Using Microbial Desalination Cells. *Environ. Sci. Technol.* **2009**, *43*, 7148–7152.
8. Kim, Y.; Logan, B. E. Microbial desalination cells for energy production and desalination. *Desalination* **2013**, *308*, 122–130.
9. Mehanna, M.; Saito, T.; Yan, J.; Hickner, M.; Cao, X.; Huang, X.; Logan, B. Using microbial desalination cells to reduce water salinity prior to reverse osmosis, *Energy. Environ. Sci.* **2010**, *3*, 1114–1120.
10. Ping, Q.Y.; Cohen, B.; Dosoretz, C.; He, Z. Long-term investigation of fouling of cation and anion exchange membranes in microbial desalination cells. *Desalination* **2013**, *325*, 48–55.
11. Jacobson, K. S.; Drew, D. M.; He, Z. Use of a Liter-Scale Microbial Desalination Cell As a Platform to Study Bioelectrochemical Desalination with Salt Solution or Artificial Seawater. *Environ. Sci. Technol.* **2011**, *45*, 4652–4657.
12. Jacobson, K.; Drew, D.; He, Z. Efficient salt removal in a continuously operated upflow microbial desalination cell with an air cathode. *Bioresour. Technol.* **2011**, *102*, 376–380.
13. Chen, X.; Xia, X.; Liang, P.; Cao, X.; Sun, H.; Huang, X. Stacked Microbial Desalination Cells to Enhance Water Desalination Efficiency. *Environ. Sci. Technol.* **2011**, *45*, 2465–2470.
14. Kim, Y.; Logan, B. Series assembly of microbial desalination cells containing stacked electro dialysis cells for partial or complete seawater desalination, *Environ. Sci. Technol.* **2011**, *45*, 5840–5845.

15. Chen, X.; Liang, P.; Wei, Z.; Zhang, X.; Huang, X. Sustainable water desalination and electricity generation in a separator coupled stacked microbial desalination cell with buffer free electrolyte circulation. *Bioresour. Technol.* **2012**, *119*, 88-93.
16. Qu, Y.; Feng, Y.; Wang, X.; Liu, J.; Lv, J.; He, W.; Logan, B. E. Simultaneous water desalination and electricity generation in a microbial desalination cell with electrolyte recirculation for pH control. *Bioresour. Technol.* **2012**, *106*, 89–94.
17. Wen, Q.; Zhang, H.; Chen, Z.; Li, Y.; Nan, J.; Feng, Y. Using bacterial catalyst in the cathode of microbial desalination cell to improve wastewater treatment and desalination. *Bioresour. Technol.* **2012**, *125*, 108–113.
18. Ge, Z.; Dosoretz, C.G.; He, Z. Effects of number of cell pairs on the performance of microbial desalination cells. *Desalination* **2014**, *341*, 101-106.
19. Zhang, B.; He, Z. Integrated salinity reduction and water recovery in an osmotic microbial desalination cell. *Rsc Adv.* **2012**, *2*, 3265-3269.
20. Yuan, H.Y.; Abu-Reesh, I.M.; He, Z. Enhancing desalination and wastewater treatment by coupling microbial desalination cells with forward osmosis. *Chem. Eng. J.* **2015**, *270*, 437-443.
21. Zhang, F.; Chen, M.; Zhang, Y.; Zeng, R. Microbial desalination cells with ion exchange resin packed to enhance desalination at low salt concentration. *J. Membr. Sci.* **2012**, *417*, 28-33.
22. Zhang, F.; He, Z. Scaling up microbial desalination cell system with a post-aerobic process for simultaneous wastewater treatment and seawater desalination. *Desalination* **2015**, *360*, 28–34.
23. El-Mekawy, A.; Hegab, H. M.; Pant, D. The near-future integration of microbial desalination cells with reverse osmosis technology, *Energy Environ. Sci.* **2014**, *7*, 3921–3933.
24. Meng, F.; Jiang, J.; Zhao, Q.; Wang, K.; Zhang, G.; Fan, Q.; Wei, L.; Ding, J.; Zheng, Z. Bioelectrochemical desalination and electricity generation in microbial desalination cell with dewatered sludge as fuel. *Bioresour. Technol.* **2014**, *157*, 120–126.
25. Zuo, K.; Cai, J.; Liang, S.; Wu, S.; Zhang, C.; Liang, P.; Huang, X. A ten liter stacked microbial desalination cell packed with mixed ion-exchange resins for secondary effluent desalination. *Environ. Sci. Technol.* **2014**, *48*, 9917–9924.
26. Esteve-Nunez, A.; Rothermich, M.; Sharma, M.; Lovley, D. Growth of *Geobacter sulfurreducens* under nutrient-limiting conditions in continuous culture. *Environ. Microbiol.* **2005**, *7*, 641–648.
27. Ortiz, J. M.; Sotoca, J. A.; Expósito, E.; Gallud, F.; García-García, V.; Montiel, V.; Aldaz, A. Brackish water desalination by electrodialysis: batch recirculation operation modeling. *J. Membr. Sci.* **2005**, *252*, 65–75.
28. Logan, B. E. *Microbial fuel cells*; Wiley-Interscience: Hoboken, N.J, 2008.
29. Malvankar, N. S.; Lovley, D. R. Microbial Nanowires: A New Paradigm for Biological Electron Transfer and Bioelectronics. *ChemSusChem* **2012**, *5*, 1039–1046.

30. Schrott, G. D.; Bonanni, P. S.; Robuschi, L.; Esteve-Núñez, A.; Busalmen, J. P. Electrochemical insight into the mechanism of electron transport in biofilms of *Geobacter sulfurreducens*. *Electrochimica Acta* **2011**, *56*, 10791–10795.
31. Fricke, K.; Harnisch, F.; Schröder, U. On the use of cyclic voltammetry for the study of anodic electron transfer in microbial fuel cells. *Energy Environ. Sci.* **2008**, *1*, 144.
32. Richter, H.; Nevin, K. P.; Jia, H.; Lowy, D. A.; Lovley, D. R.; Tender, L. M. Cyclic voltammetry of biofilms of wild type and mutant *Geobacter sulfurreducens* on fuel cell anodes indicates possible roles of OmcB, OmcZ, type IV pili, and protons in extracellular electron transfer. *Energy Environ. Sci.* **2009**, *2*, 506.
33. Robuschi, L.; Tomba, J. P.; Schrott, G. D.; Bonanni, P. S.; Desimone, P. M.; Busalmen, J. P. Spectroscopic Slicing to Reveal Internal Redox Gradients in Electricity-Producing Biofilms. *Angew. Chem. Int. Ed.* **2013**, *52*, 925–928.
34. Bonanni, P. S.; Bradley, D. F.; Schrott, G. D.; Busalmen, J. P. Limitations for Current Production in *Geobacter sulfurreducens* Biofilms. *ChemSusChem* **2013**, *6*, 711–720.
35. Esteve-Núñez, A.; Busalmen, J. P.; Berná, A.; Gutiérrez-Garrán, C.; Feliu, J. M. Opportunities behind the unusual ability of *Geobacter sulfurreducens* for exocellular respiration and electricity production. *Energy Environ. Sci.* **2011**, *4*, 2066.
36. Esteve-Núñez, A.; Sosnik, J.; Visconti, P.; Lovley, D. R. Fluorescent properties of c-type cytochromes reveal their potential role as an extracytoplasmic electron sink in *Geobacter sulfurreducens*. *Environ. Microbiol.* **2008**, *10*, 497–505.
37. Ping, Q.; Porat, O.; Dosoretz, C. G.; He, Z., Bioelectricity inhibits back diffusion from the anolyte into the desalinated stream in microbial desalination cells, *Water Res.* **2016**, *8*, 266-273.
38. Cerci, Y.; Cengel, Y.; Wood, B.; Kahraman, N.; Karakas, E.S. Improving the Thermodynamic and Economic Efficiencies of Desalination Plants: Minimum Work Required for Desalination and Case Studies of Four Working Plants, *Desalination and Water Purification Research and Development Program Final Report No. 78, University of Nevada* **2003**. (<https://www.usbr.gov/research/AWT/reportpdfs/report078.pdf>)
39. Liu, F.; Ouedraogo, A.; Manghee, S.; Danilenko, A. A Primer on Energy Efficiency for Municipal Water and Wastewater Utilities, *Energy Sector Management Assistance Program - The World Bank* **2012**. (<http://www.ifc.org>)
40. Mehanna, M.; Kiely, P. D.; Call, D. F.; Logan, B. E. Microbial electro dialysis cell for simultaneous water desalination and hydrogen gas production. *Environ. Sci. Technol.* **2010**, *44*, 9578–9583.
41. Ping, Q.Y.; He, Z. Effects of inter-membrane distance and hydraulic retention time on the desalination performance of microbial desalination cells. *Desalin. Water Treat.* **2014**, *52*, 1324-1331.

42. Ghadge, A.N.; Jadhav, D. A.; Pradhan, H.; Ghangrekar, M. M., Enhancing waste activated sludge digestion and power production using hypochlorite as catholyte in clayware microbial fuel cell, *Bioresource Technol.* **2015**, *18*, 225–231.